Merocyanines in a Halogen-Bonded Network Involving Inorganic Building Blocks

Seiler, Vanessa K.; Tumanov, Nikolay; Robeyns, Koen; Champagne, Benoît; Wouters, Johan; Leyssens, Tom

Published in:
Crystal Growth and Design

DOI:
10.1021/acs.cgd.9b00903

Publication date:
2020

Document Version
Publisher's PDF, also known as Version of record

CRYSTAL GROWTH & DESIGN

Article

Cite This: Cryst. Growth Des. 2020, 20, 608−616

pubs.acs.org/crystal

Merocyanines in a Halogen-Bonded Network Involving Inorganic Building Blocks

Vanessa K. Seiler,[†] Nikolay Tumanov,[‡] Koen Robeyns,[†] Benoit Champagne,[‡] Johan Wouters,[‡] and Tom Leyssens*[,†]

[†]IMCN Institute of Condensed Matter and Nanosciences, Université catholique de Louvain, Place Louis Pasteur 1, 1348 Louvain-la-Neuve, Belgium

[‡]Chemistry Department, University of Namur, Rue de Bruxelles 61, 5000 Namur, Belgium

Supporting Information

ABSTRACT: In this work, we present spiropyran derivatives (SP) involving a halogen bonded network with the addition of inorganic building blocks, i.e. inorganic acids and bivalent metal salts. In solution, a ring-opening isomerization of the spiropyran results in the colored merocyanine isomer (MC), which is only rarely observed in the solid state. By detaining the phenolate oxygen atom of the merocyanine in a hydrogen (HB) or halogen bond (XB) we can successfully obtain this form and access a variation in chromic properties. The O atom of the open MC form unfortunately only represents a weak XB acceptor which led us to introduce supplementary building blocks to strengthen this type of interaction. Fourteen new crystal forms were determined with 3 spiropyran derivatives (1,3,3-trimethylindolinospiropyran (**SPH/MCH**), 1,3,3-trimethylindolino-6′-nitrobenzopyrylospiran (**SPNO2/MCNO2**), 1,3,3-trimethylindolino-β-naphthopyrylospiran (**SPBenz/MCBenz**)) and several di- and tritopic XB donors (1,3,5-triiodotrifluorobenzene (135tfib), 1,4-diiodotetrafluorobenzene (14tfib), 1,3-diiodotetrafluorobenzene (13tfib), 1,2-diiodotetrafluorobenzene (12tfib), abd 1,2-diiodotetrafluoroethan (12tfe)) as well as a polymorphic form of the parent compound with hydrochloric acid. We successfully expanded the XB interaction possibilities with hydrochloric acid or zinc/cobalt chloride and found proof of the tunability of the chromic properties in the solid state using these building blocks.

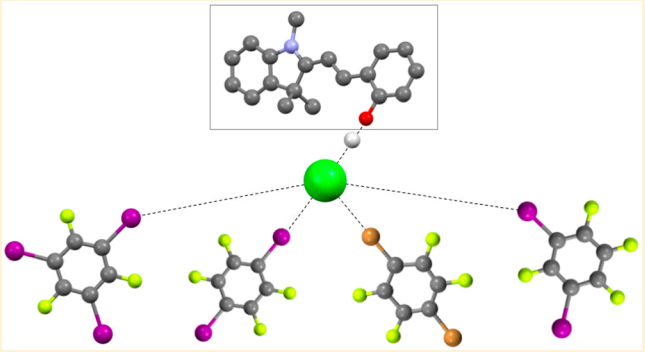

INTRODUCTION

Salt formation and cocrystallization are the most often applied solid-state approaches for the systematic modification of the solid form of pharmaceutical materials.[1−4] It also has become an accepted way of modifying the physical and chemical properties not only for drug compounds but also in other research areas such as molecular semiconductors,[5] protein-nucleic acid complexation[6] and organic dyes.[7,8] As an example, anil derivatives—since 1939, widely studied photochromic compounds[9−14]—have been shown to be impacted by cocrystallization[15−18] for altering their photochromic character.[19,20] Also spiropyrans (SP) are photochromic compounds showing a broad color array according to the nature of the compound. For these compounds, light irradiation can lead to an isomeric transition from a closed SP form, which is usually uncolored, to a deeply colored open form, called merocyanine (MC).[21−25] This isomerization is impacted by temperature or irradiation with a specific wavelength[26,27] and has been mostly observed in solution. Only in rare occasions does one encounter the open, colored MC form in the solid state.[28] Typically, only the spiropyran form crystallizes from solution independent of the parent composition in solution. Achieving the open form at the solid-state can be interesting for color-based applications. The goal of the current work was to use crystal engineering principles to come to a stabilization of the MC form and an associated deep coloration of the solid to apply the stabilized merocyanine to halogen bonding. To achieve this objective, we aimed for a cocrystallization approach and stabilize the open form via intermolecular interactions. As the spiropyran compounds inherently have only a limited number of hydrogen bonding acceptor or donor sites,[29] we turned to halogen bonding (XB) as an alternative stabilization tool for the open MC form. Despite tackling the same acceptor site of the spiropyran/merocyanine for both type of interactions, halogen bonding allows the spiropyran to act as donor site also and increases the variety of possible intermolecular interactions. The halogen bond is similar to a hydrogen bond, but its strength depends on the surrounding of the halogen atom and the basicity of the donor site.[30,31] It is described by its very directional character and varying interaction lengths.[32]

Received: July 10, 2019
Revised: November 28, 2019
Published: December 19, 2019

DOI: 10.1021/acs.cgd.9b00903
Cryst. Growth Des. 2020, 20, 608−616

Scheme 1. Overview of the Approach Used Here, with XB as a Tool To Stabilize the MC[a]

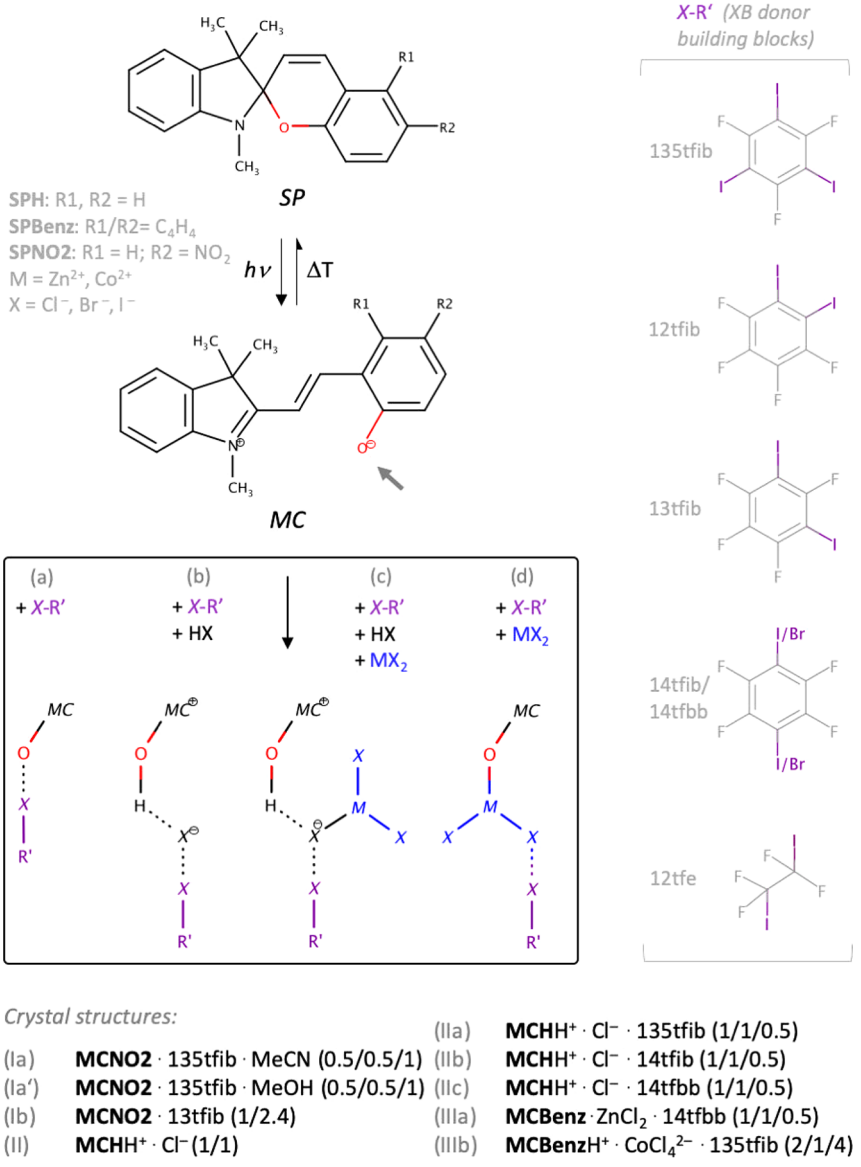

[a]Additional XB building blocks are introduced starting from spiropyran salts or complexes.

At first, we target the $-NO_2$ group of 1,3,3-trimethylindolino-6′-nitrobenzopyrylospiran (**SPNO2/MCNO2**) as a halogen bond acceptor leading to a possible stabilization of the colored MC form. The advantage is not only the halogen interaction possibility via the nitro group but also with the phenolate oxygen atom of the merocyanine form. In a second approach we want to open halogen bonding possibilities for those spiropyrans not containing such a nitro group and leaving the phenolate oxygen as sole position to tackle (i.e., 1,3,3-trimethylindolinospiropyran (**SPH/MCH**) and 1,3,3-trimethylindolino-β-naphthopyrylospiran (**SPBenz/MCBenz**)). To do so, we introduce inorganic building blocks (Cl^-, $ZnCl_2$, $CoCl_2$) by salt formation[33,34] or complexation,[35] which are shown as suitable XB acceptors in ionic[36−38] and neutral metal organic complexes.[39,40] We then take this intermediate form and introduce appropriate XB donors to form multicomponent systems. The inorganic building block plays a key role in the stabilization of the merocyanine form, whereas the halogen bond donor forms intermolecular interactions to this unit. Combining complexation/salt formation with XB cocrystallization, we are able to obtain a multicomponent crystalline system, that stabilizes the MC form and leads to strongly colored halogen bonded products (Scheme 1). These materials were successfully prepared and shown to not only be accessible through a traditional solvent based approach but also using a mechanochemical approach.

EXPERIMENTAL SECTION

Materials. All compounds were commercially available and used without further purification (Spiropyrans from TCI Chemicals; 1,3,5-trifluoro-2,4,6-triiodobenzene, 1,4-diiodotetrafluorobenzene, 1,4-diiodotetrafluorobenzene from FluoroChem; 1,4-dibromotetrafluorobenzene from Sigma-Aldrich; 1,2-diiodotetrafluoroethan from Alfa aesar; cobalt chloride hexahydrate and zinc chloride from Fisher). Applied solvents were of reagent grade and hydrochloric acid was applied as aqueous solution (12.1 M).

Synthesis and Crystallization. All single crystals were obtained by isothermal (room temperature) solvent evaporation from various solvents. Here, 10−20 mg of the components in total were mixed in

DOI: 10.1021/acs.cgd.9b00903
Cryst. Growth Des. 2020, 20, 608−616

Table 1. Crystallographic Details for Crystal Structures Ia−IIIb

	Ia	Ia′	Ib	II	IIa
chemical formula	$0.5(C_{19}H_{18}N_2O_3)$, $0.5(C_6F_3I_3)$, C_2H_3N	$0.5(C_{19}H_{18}N_2O_3)$, $0.5(C_6F_3I_3)$, CH_4O	$C_{19}H_{18}N_2O_3$, $2.38(C_6F_4I_2)$	$C_{19}H_{20}NO{\cdot}Cl$	$C_{19}H_{20}NO{\cdot}Cl$ $0.5(C_6F_3I_3)$
M_r (g mol^{-1})	873.17	864.15	1280.58	313.81	568.69
crystal system, SG	orthorhombic, *Pnma*	orthorhombic, *Pnma*	orthorhombic, *Pnma*	orthorhombic, *Cmca*	monoclinic, *C*2/*c*
temperature (K)	293(2)	295(2)	295(2)	295(2)	100(2)
a, *b*, *c* (Å)	25.776(3), 6.9892(8), 16.0234(17)	25.2771(3), 6.97493(11), 15.9522(2)	34.4987(12), 6.89385(18), 16.1070(3)	6.92445(19), 31.0415(7), 15.2037(3)	43.6782(9), 13.8458(3), 6.98463(14)
α, β, γ (deg)	90, 90, 90	90, 90, 90	90, 90, 90	90, 90, 90	90, 94.1865(19), 90
V (Å^3)	2886.7(6)	2812.46(6)	3830.71(18)	3267.97(14)	4212.73(16)
Z	4	4	4	8	8
μ (mm^{-1})	3.301 (Mo Kα)	26.668 (Cu Kα)	31.168 (Cu Kα)	2.066 (Cu Kα)	19.086 (Cu Kα)
crystal size (mm)	0.30 × 0.03 × 0.01	0.390 × 0.043 × 0.020	0.370 × 0.028 × 0.012	0.360 × 0.058 × 0.018	0.490 × 0.029 × 0.021
crystal color/shape	red needle	red needle	red needle	yellow needle	orange needle
$R[F^2 > 2\sigma(F^2)]$, $wR(F^2)$, *S*	0.050, 0.087, 1.04	0.029, 0.079, 1.11	0.047, 0.124, 1.06	0.033, 0.089, 1.04	0.035, 0.096, 1.11
$\Delta\rho_{max}$, $\Delta\rho_{min}$ (e Å^{-3})	0.65, −0.58	1.49, −0.68	0.94, −0.79	0.21, −0.17	1.31, −0.76
CCDC no.	1917493	1917494	1917495	1917496	1917497

	IIb	IIc	IIIa	IIIb
chemical formula	$C_{19}H_{20}NO{\cdot}Cl$ $0.5(C_6F_4I_2)$	$C_{19}H_{20}NO{\cdot}Cl$ $0.5(C_6F_4Br_2)$	$C_{23}H_{21}NOCl_2Zn$, $0.5(C_6Br_2F_4)$	$2(C_{23}H_{22}NO){\cdot}Cl_4Co$ $4(C_6F_3I_3)$
M_r (g mol^{-1})	514.74	935.50	617.62	2896.60
crystal system, SG	monoclinic, *C*2/*c*	monoclinic, *C*2/*c*	monoclinic, $P2_1/c$	monoclinic, $P2_1/n$
temperature (K)	297(2)	295(2)	100(2)	297(2)
a, *b*, *c* (Å)	43.4343(10), 13.5885(3), 7.17910(15)	43.0611(15), 13.5192(8), 7.0996(4)	9.27926(13), 13.18720(19), 19.7346(3)	18.5008(4), 19.8288(4), 22.3323(6)
α, β, γ (deg)	90, 92.313(2), 90	90, 92.349(4), 90	90, 92.0387(14), 90	90, 90.800(2), 90
V (Å^3)	4233.69(17)	4129.6(4)	2413.35(6)	8191.8(3)
Z	8	4	4	4
μ (mm^{-1})	1.668 (Mo Kα)	4.166 (Cu Kα)	5.701 (Cu Kα)	4.934 (Mo Kα)
crystal size (mm)	0.30 × 0.07 × 0.05	0.400 × 0.047 × 0.018	0.230 × 0.190 × 0.120	0.30 × 0.12 × 0.08
crystal color/shape	red rod	orange needle	orange block	red block
$R[F^2 > 2\sigma(F^2)]$, $wR(F^2)$, *S*	0.034, 0.076, 1.05	0.0733, 0.20, 1.10	0.028, 0.071, 1.07	0.034, 0.088, 1.10
$\Delta\rho_{max}$, $\Delta\rho_{min}$ (e Å^{-3})	0.50, −0.31	0.85, −0.46	0.65, −0.55	2.18, −1.23
CCDC no.	1917498	1917499	1917500	1917501

DOI: 10.1021/acs.cgd.9b00903
Cryst. Growth Des. 2020, 20, 608−616

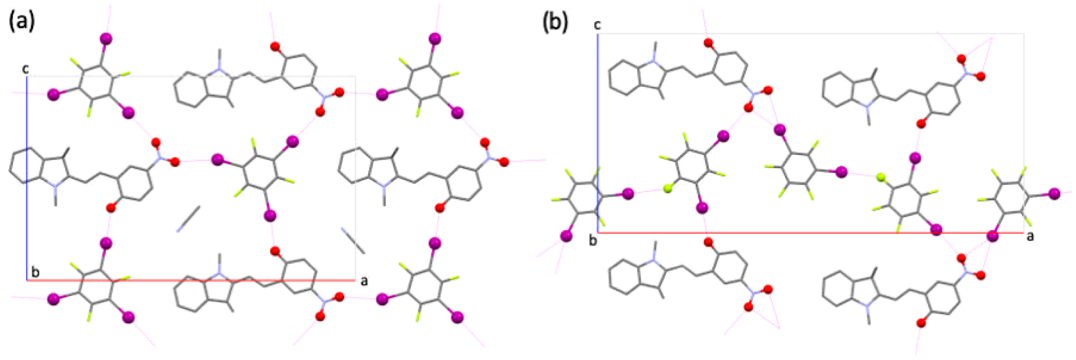

Figure 1. (a) Partial packing diagram of **MCNO2** with the XB donor 135tfib (**Ia**) showing the cavity occupied by solvent molecules of MeCN, and (b) the crystal structure of **MCNO2** with 13tfib (**Ib**) not displaying the disordered XB donor. XBs are indicated as dashed lines.

an equimolar ratio or at molar ratio of 2:1 in accordance with the composition of the crystal and dissolved completely. If necessary, the samples were heated close to the boiling point of the respective solvent to accelerate the dissolution process (**Ib**, **IIa** in ethanol; **Ia′** in methanol; **Ia**, **IIIb** in acetonitrile; **II**, **IIb**, **IIc**, **IIIa** in acetone). See detailed composition in Table S1.

Single Crystal Data Collection and Refinement. Crystal data, data collection, and refinement details are given in Table 1.

Single crystal X-ray diffraction data for **Ia**, **IIb**, and **IIIb** were collected on a MAR354 image plate using Mo Kα radiation (rotating anode Rigaku UltraX 18S, Xenocs Fox3D mirrors). In the case of **Ia′**, **Ib**, **II**, **IIa**, **IIc**, and **IIIa**, data were collected on an Oxford Diffraction Gemini Ultra diffractometer (Ruby CCD detector) using Mo Kα or Cu Kα radiation. Data reduction was carried out using the CrysAlisPro software package,[41] and the implemented absorption correction was applied. The crystal structures were solved using SHELXT and refined by full-matrix least-squares refinement on IFI^2 (SHELXL-2014[42]). Non-hydrogen atoms were treated anisotropically. C-bound hydrogen atoms were placed in calculated positions and refined using a riding model with isotropic displacement parameters set to $1.2U_{eq}(C)$ of the parent atoms for secondary and aromatic hydrogen atoms and $U_{iso}(H) = 1.5U_{eq}(C)$ for methyl hydrogens. Free rotation about the local 3-fold axis was allowed for all methyl groups. Symmetry analysis and validation was carried out using PLATON.[43] Molecular graphics were created using Mercury.[44]

In **Ia′**, the MeOH molecule is disordered over two positions, which results from its special position on a mirror plane in a cavity with no stabilizing directional interactions.

Liquid-Assisted Grinding (LAG) and X-ray Powder Diffraction (XRPD). For liquid-assisted grinding experiments, approximately 30−50 mg of total compound was mixed in a molar ratio in accordance to the composition of the respective crystal structure in 2 mL Eppendorf tubes in the presence of 5−10 μL of acetone and ground for 10−15 min in a Retsch MM400 Mixer mill at 30 Hz with two stainless steel balls (o.d. 2 mm) in each tube. The resulting powders were analyzed by X-ray powder diffraction measurements on a Panalytical X'Pert PRO diffractometer operating at 45 kV and 30 mA (linear X'Celerator detector) or on a Siemens D5000 diffractometer (40 kV and 40 mA; point scintillation detector) using Cu Kα radiation at room temperature in the 2θ range of 2/4−40° and reflection mode over a flat sample. The Mercury program[44] was used for calculation of theoretical X-ray powder patterns from single crystal structure data.

Diffuse Reflectance Spectroscopy (DRS). Measurements were performed on a Varian 5000 UV/vis/NIR spectrometer. To avoid matrix effects, pure powder was used for measurements and subsequently converted to absorption spectra using the Kubelka−Munk function. The scan was plotted in a wavelength range between 800 and 200 nm with an interval of 1 nm and an average exposure time of 0.1 s. Data are normalized to a value of 1 and a correction factor was applied to compensate a jump-shift around 350 nm caused by the setup.

RESULTS AND DISCUSSION

Spiropyrans and XBs. In a first approach, we investigated the possibility of directly stabilizing the MC form using XB. Typical XB donors contain an aromatic ring with complete replacement of the H atoms by halogen atoms.[45,46] Usually I or Br atoms are the main XB donors with F atoms at the remaining positions. Using this approach, the XB bond targeted here is of the R-X $\cdots O^-$ form. However, cocrystallization turned out to be unsuccessful for **SPH** and **SPBenz** derivatives, showing the $O_{MC}\cdots X-R$ halogen bond not strong enough to stabilize the open MC form at the solid state if no additional interaction site is present. In the case of **SPNO2**, however, cocrystal formation is observed and can be attributed to the additional XB sites offered by the NO_2 functional group.[47] The halogen atom can either form a monocoordinate interaction with one of the nitro O atoms or a bifurcated interaction when involving both nitro O atoms.[48]

Co-crystallization experiments with **SPNO2** from solution, revealed three new cocrystal forms (Figure 1, Figure S1). In all cases the XB occurs between the I atom and the phenolate O atom and either one or both nitro O atoms ($O_{MCNO2}\cdots I-R'$). **Ia** and **Ia′** form isostructural cocrystal solvates with half a **MCNO2** and half a 135tfib molecule in the asymmetric unit placed on a mirror plane in the space group *Pnma*. The cavities formed by the shifted layer like arrangement of the main molecules are occupied by solvent molecules (MeCN in the case of **Ia** and MeOH for **Ia′**). The solvent molecules show large thermal displacement factors, characteristic for solvent molecules trapped in available cavities without any directional interaction. For the methanol solvate, two positions of the disordered solvent molecule were modeled. **Ib** crystallizes in the space group *Pnma* with **MCNO2** and 13tfib molecules located on a mirror plane. The nitro group of **MCNO2** forms a bifurcated halogen bond with one I atom of 13tfib each. The second I atom in turn extends the network via a $R'-I\cdots F-R'$ XB to a second 13tfib molecule. The phenolate O atom of **MCNO2** is also involved in a XB with the I atom of a 13tfib molecule, which also connects to the nitro O atom of a symmetry equivalent **MCNO2** outside the asymmetric unit. These interactions form a 2-dimensional network as in **Ia**/**Ia′** resulting in an overall layer like arrangement.

Introducing Supplementary Building Blocks for Preferred XBs. To cocrystallize merocyanine forms of spiropyran compounds not containing a nitro-group such as **SPH**/**MCH** and **SPBenz**/**MCBenz** we took a crystal engineering approach, trying to introduce additional XB building blocks to the system. As shown in our previous work,[33,35] the

DOI: 10.1021/acs.cgd.9b00903
Cryst. Growth Des. 2020, 20, 608−616

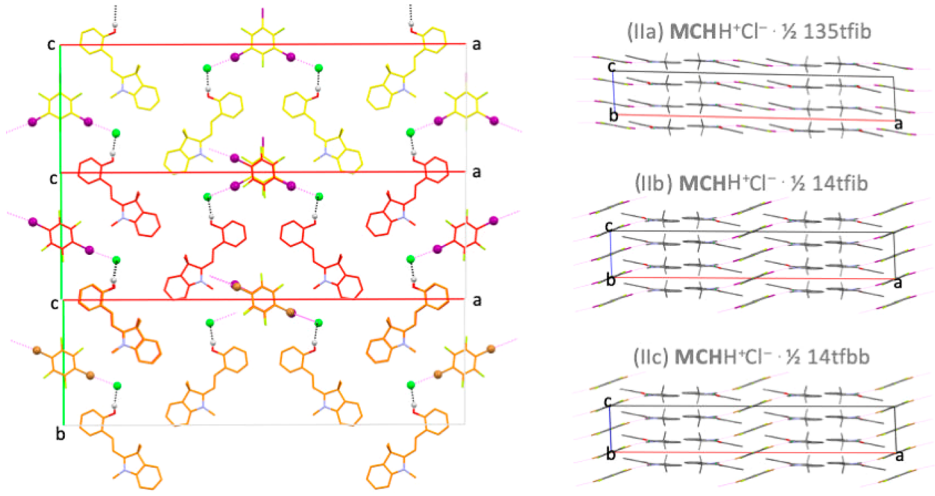

Figure 2. Left: Partial packing diagram of **IIa** yellow C atoms, **IIb** red C atoms, and **IIc** orange C atoms in an overlay showing each **MCH**H^+Cl^- with one XB donor connected to the Cl^- ion. Right: Partial packing diagram displayed along the *b*-axis of **IIa**–**IIc**. HBs are indicated as black dashed lines and XBs in violet.

merocyanine form of spiropyran compounds form salts and complexes with inorganic acids and metal salts, respectively. This formation allows introducing halogen anions such as Cl^-, which could potentially be used to construct XBs. So instead of starting from the **SPH** and **SPBenz** compounds, we decided to investigate halogen bonding starting from the respective spiropyran salt ((MC)H^+Cl^-) and (MC)$ZnCl_2$ complex, with the idea to create a halogen bond "bridge" between the merocyanine and the XB donors.

This idea turned out to be successful, as crystallization experiments between **SPH** and the XB donors in the presence of hydrochloric acid resulted in five new forms, three of which were structurally determined **IIa**–**IIc**. Tri- and ditopic XB aromatic coformers with respectively I or Br atoms aromatic ring were selected for these experiments. **IIa**, **IIb**, and **IIc** crystallize in the monoclinic space group *C*2/*c* with one protonated merocyanine and half a XB donor placed on an inversion center in the asymmetric unit (Figure 2).

All crystal structures show protonation of the oxygen atom, leading to a $O_{MC}{}^-H^+\cdots Cl^-$ charge-assisted hydrogen bond stabilizing the merocyanine form as observed previously.[33] In **IIa** and **IIb**, a XB from the donor 135tfib or 14tfib is formed between the I atom and the Cl^- ion. In **IIc**, the same type of interaction is formed between the Cl^- ion and the Br atom resulting in a form isomorphous of **IIb**. Despite the different topicity of the XB donors, the resulting structures are highly similar showing sheets of protonated merocyanine ions along the *ab*-layer. 135tfib serves as connective link within the layer whereas 14tfib and 14tfbb cross-link the different layers. The bonding pattern O–H $\cdots X^-\cdots X'$–R′ is presented by the unbound and negatively charged halide ion in the role of a bridging element for any halogen atom opposed by an O–H unit as revealed by a CSD[49] search. Whereas the halide ion as general XB building unit of the form R′–X $\cdots X^-\cdots X'$–R″ was found before,[50] only six hits were obtained (Refcodes: GUYNIZ,[50] GUYNOF,[50] IFULEC,[51] RUWVUB,[52] RUWWIQ,[52] YORZUC[53]) showing the O–H $\cdots X^-\cdots X'$–R′ interaction. In five of these structures, the polytopic halide ion either forms a XB with the I atom or an HB with the hydroxy group of a solvent molecule, i.e. ethanol, methanol, or H_2O. Only in the latter structure the interaction to a protonated organic molecule is present as shown here.

The materials presented here can be obtained using multiple pathways. While the single crystals were obtained from solution through solvent evaporation of a saturated solution, pure bulk material was also obtained by a mechanochemical approach. After forming the precursor **MCH**H^+Cl^- from solution the product is used in a liquid-assisted grinding (LAG) approach with the XB donor in a molar ratio in accordance to the composition. With an experimental grinding time of only 10–15 min, a complete conversion can be achieved. Subsequent XRPD analysis showed the formation of the (ionic) cocrystal. In Figure 3, a comparison of the powder patterns calculated from the single crystal data with the experimental XRPD patterns of the products obtained through the mechanochemical approach is shown for **IIa**–**IIc**. In all cases the XRPD patterns match, proving that the material can be prepared by either method. This latter method is simple, fast and leads to complete conversion without the need of a solution-based system containing all components. For 12tfib and 12tfe, the mechanochemical approach shows formation of new solid-state forms for which no structural information by SC-XRD could be obtained (Figure S2). Respective solvent evaporation experiments solely resulted in a new Polymorph of **MCH**H^+Cl^- (Figure S3).

Similarly, the LAG approachstarting from **MCBenz**H^+Cl^- shows new solid forms when using the 14tfib, 12tfib, and 12tfe coformers (Figure S4). We were unsuccessful to obtain these from solution, likely due to the low solubility of **MCBenz**H^+Cl^- in the tested solvents.

The halogen bonds formed between the phenolate oxygen of the merocyanine and the iodine of the halogen bond donors in structures **Ia**/**Ia′** and **Ib** show a strong interaction with a difference of the van der Waals radii of around −0.70 Å to the respective atoms and a nearly linear arrangement for C–I$\cdots$O (Table S2). The halogen bonds directed toward the nitro group are less directional with a difference in van der Waals radii of only −0.15 up to −0.44 Å. Furthermore, the interactions formed between the chlorine and iodine in structures **IIa**, **IIb**, and **IIc** with the inorganic building blocks present have similar differences of approximately −0.5 Å

DOI: 10.1021/acs.cgd.9b00903
Cryst. Growth Des. 2020, 20, 608–616

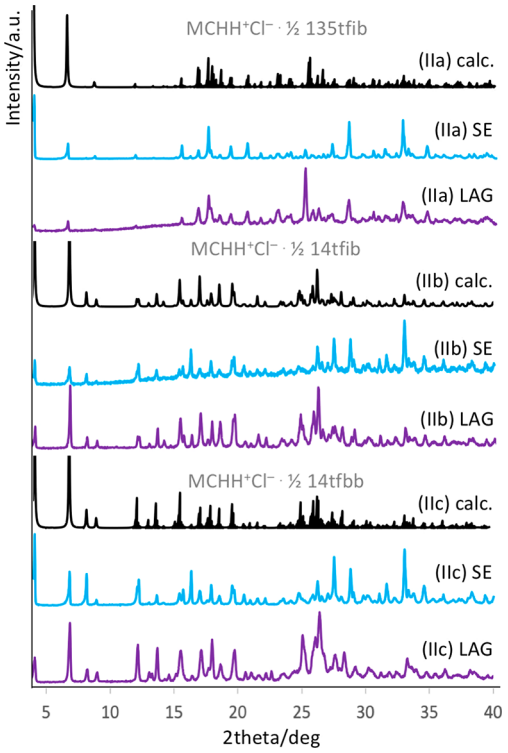

Figure 3. Overlay of XRPD patters for **IIa**, **IIb**, and **IIc**. The XRPD pattern calculated from single crystal data are compared to experimental XRPD pattern by solvent evaporation (SE) and liquid-assisted grinding (LAG).

compared to the direct halogen bond of the iodine to the merocyanine.

Spiropyran metal-based complexes/salts also turned out to be successful intermediates toward multicomponent XB solid forms and an alternative to the (MC)H^+Cl^- approach. On the basis of the different linking possibilities of bivalent metal salts with spiropyran derivatives (i.e., complexation with an O_{MC}-MX_2 bond or salt formation with a charge-assisted hydrogen bond O_{MC}–$H^+\cdots X^-$–MX_2)[35] two examples of each involving a halogen bonding are presented in this work. The halogen bonded complex of **MCBenz**,(IIIa), coordinating to $ZnCl_2$ forms a Cl···Br halogen bond to both Br atoms on either side of 14tfbb. First, the complex of the spiropyran with the metal salt is formed in solution and crystallizes then with the XB donor in the space group $P2_1/c$ with one spiropyran metal unit and half of the XB donor in the asymmetric unit (Figure 4a). The second example is given by the salt of **MCBenz** with $CoCl_2$ which crystallizes with 135tfib ((IIIb), Figure 4c) from the same pot. The multicomponent compound crystallizes in the monoclinic space group $P2_1/n$ with two protonated **MCBenz** ions, one $[CoCl_4]^{2-}$ unit and four 135tfib halogen bond donors in the asymmetric unit (Figure 4c). The I atoms of three of the 135tfib molecules form an XB to either one of the Zn-coordinated chloride ligands. In addition, XBs between the iodine atoms of XB coformers in function of acceptors and donors result in a 3-dimensional network.

As shown before for MCH^+Cl^-, solvent evaporation of the acetone solvate of **MCBenz**$ZnCl_2$ with 14tfbb as well as LAG experiments in the presence of acetone result in the cocrystal **IIIa** proving both as a suitable approach to obtain this form (Figure 4b). Furthermore, a new solid form could be identified from the LAG experiment between **MCBenz**$ZnCl_2$ and 12tfe (Figure S5), but so far, we were unsuccessful in determining the crystal structure of this form. Due to the lack of pure bulk material of the protonated **MCBenz** compound with cobalt chloride, operability of the solid-state approach remains part of ongoing research. Nevertheless, the interaction of **SPBenz** with cobalt chloride forming a salt is proven for the first time by the structure determination of **IIIb**.

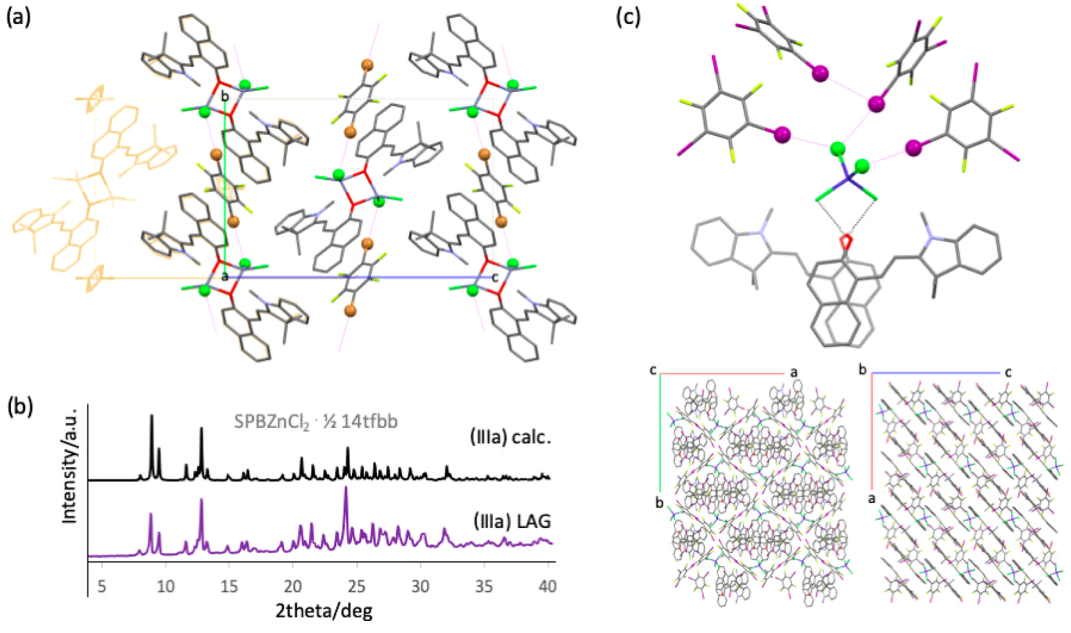

Figure 4. (a) Partial packing diagram of **IIIa** in comparison to the parent complex **MCBenz**$ZnCl_2$ crystallizing with acetone. (b) Comparison of the XRPD patterns calculated from single crystal data **IIIa** and those obtained of the product by LAG. (c) Asymmetric unit of **IIIb** showing the multicomponent solid formation comprised of **MCBenz**, $[CoCl_4]^{2-}$ and 135tfib. Two different perspectives are highlighted below. HBs are indicated as black dashed lines and XBs in purple.

DOI: 10.1021/acs.cgd.9b00903
Cryst. Growth Des. 2020, 20, 608–616

Diffuse Reflectance Spectroscopy—Impact of the XB on the UV–Vis Absorption Properties. To study the chromic properties of all spiropyran-halogen bonded solids, diffuse reflectance spectroscopy was performed. The closed spiropyran form of the yellow colored **SPNO2** shows absorption between 200 and 470 nm due to charge transfer $\pi-\pi^*$ electronic transitions between the phenolate and indoleninium of the molecule as represented by the gray curve in Figure 5a. The delocalization of the π-electrons throughout the whole molecule by the ring-opening isomerization leads typically to strong absorption in the visible range, which has already been shown in solution.[54] The cocrystal of **MCNO2** with 135tfib **Ia**) reflects these changes of the absorption properties in the solid state with absorption maxima up to 670 nm resulting in a strongly red colored powder (purple curve in Figure 5a). Unfortunately, no pure bulk material of **MCNO2** with 13tfib (**Ib**) was obtained for detailed UV/vis analysis, though visual inspections of the single crystal showed a similar red coloration compared to 135tfib (Figure S6).

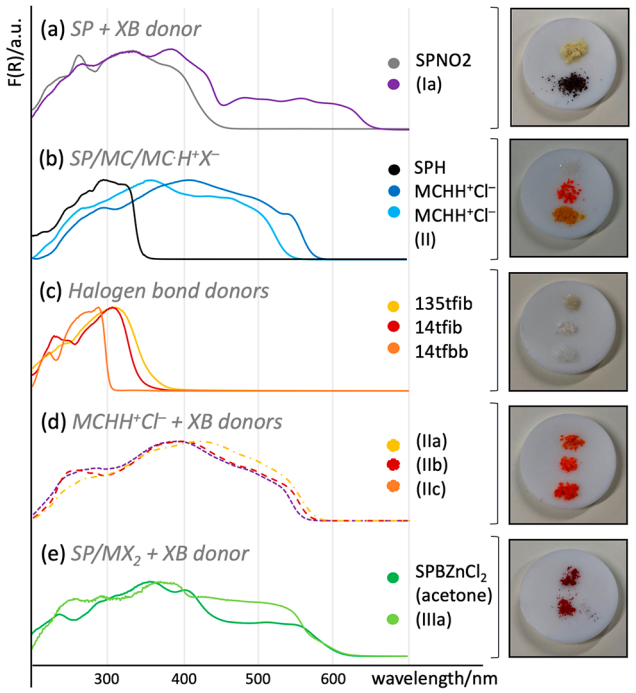

Figure 5. Diffuse reflectance spectroscopy measurements of (a) the cocrystal **Ia** of **MCNO2** with 135tfib compared to **SPNO2** (top; purple and gray curve). (b) **SPH** in its closed spiropyran form in comparison with the two polymorphs of the salt formed with hydrochloric acid (black and blue curves). (c) Absorption of the XB donor coformers alone (yellow to red curves). (d) Absorption spectra of **Ia**, **Ib**, and **Ic** (dotted yellow to red curves) with the absorption spectra. (e) Differences between the **MCBenz**$ZnCl_2$ acetone solvate and the respective crystal (**IIIa**) with 14tfbb replacing the acetone in the crystal unit. Photos of the bulk materials are depicted on the left of each spectral data.

The multicomponent crystals of **MCH**H^+Cl^- with halogen bond donors **IIa**–**IIc** display a coloration similar to the **MCH**H^+Cl^- compound as illustrated in Figure 5d (red/orange and yellow dashed lines). The absorption extending up to 570/590 nm shows similar bathochromic shifts and high similarities to the parent **MCH**H^+Cl^-, whereas the spiropyran form of **SPH** only shows absorption up to 400 nm (black curve Figure 5b). It can be expected that the protonation of the merocyanine restricts the donor character of the charge transfer $\pi-\pi^*$ electronic transition, which is responsible for the color. Therefore, different types of XB interactions of this unit only have a negligible effect on the color of the solid.

The solid-state material made of the metal-containing multicomponent system (**IIIa**) has UV/vis characteristics fairly similar to those of the parent acetone solvate of **MCBenz**$ZnCl_2$ both showing absorptions up to 600 nm (green curves in Figure 5e). Nevertheless, despite the similar wavelength range of absorption between the Zn-complex of **MCBenz** and this multicomponent XB complex, significant differences were found regarding the position of absorption maxima. This indicates an influence of the XB donor interaction forwarded via the metal unit toward the spiropyran and affecting the chromic properties.

Footnote. "The polymorphs of **MCH**H^+Cl^- show slightly difference color properties with respect to each other. While it was already stated that the previously known polymorph is deeply orange colored showing absorption maxima up to 590 nm, diffuse reflectance spectroscopy confirmed a yellow coloration for the newly discovered polymorph (**II**) with absorption up to 570 nm (blue curves in Figure 5b). "

CONCLUSION

In this contribution, we present a novel approach to the stabilization of the merocyanine form of spiropyrans at the solid state, through introduction of halogen bonding. A direct two component cocrystallization of the merocyanine form with a XB donor is only feasible with the nitro substituted derivative **SPNO2** as XB interactions occur with the nitro group as well as the observation of an $O_{MC}\cdots X-R'$ halogen bond including the phenolate oxygen of the merocyanine. When only this latter interaction is possible (**SPH**, **SPBenz**) two component cocrystallization is not observed with halogen bonding as suitable stabilization of the merocyanine form. We therefore successfully introduced a crystal engineering approach to expand the possibilities for XB interactions, starting not from the spiropyran compounds, but rather from their respective (MC)H^+Cl^- salts and (MC)$ZnCl_2$ complexes, which are previously stabilized with inorganic building blocks. This successfully led to multicomponent cocrystal formation with XB donors using either a solution or mechanochemical approach. The multicomponent cocrystals based on (MC)-H^+Cl^- show O_{MC}-$H\cdots X^-\cdots X-R'$ XBs built via the counterion stabilizing the protonated merocyanine in a charge-assisted HB providing a preferable XB acceptor. The stabilization of the merocyanine via the protonation of the phenolate oxygen unfortunately restricts the influence on the chromic properties by enclosing the π-electron system. Starting from the merocyanine metal salt an $O_{MC}-H\cdots X_2MX\cdots X-R'$ bonding pattern could be observed with the chlorine ligand serving as XB acceptor ($O_{MC}-MX_2\cdots X-R'$). This method shows a significant influence on the UV/vis absorption characteristics presenting XBs as a suitable tool to alter the solid-state properties of spiropyran compounds. The approach presented in this contribution, therefore, shows how crystal engineering is used to stabilize the merocyanine form via halogen bonding at the solid state and how halogen bonded multicomponent systems can be created by choosing the appropriate starting material, obtaining a flexibility in the coloration of these compounds at the solid state.

DOI: 10.1021/acs.cgd.9b00903
Cryst. Growth Des. 2020, 20, 608–616

■ ASSOCIATED CONTENT

Supporting Information

The Supporting Information is available free of charge at https://pubs.acs.org/doi/10.1021/acs.cgd.9b00903.

Partial packing diagram of **Ia′**, composition of the crystallization experiments for slow solvent evaporation, XRPDs, structural details of **II**, partial packing diagram of **II**, picture of the single crystal of **Ib**, and halogen bond overview bond lengths and angles (PDF)

Accession Codes

CCDC 1917493−1917501 contain the supplementary crystallographic data for this paper. These data can be obtained free of charge via www.ccdc.cam.ac.uk/data_request/cif, or by emailing data_request@ccdc.cam.ac.uk, or by contacting The Cambridge Crystallographic Data Centre, 12 Union Road, Cambridge CB2 1EZ, UK; fax: +44 1223 336033.

■ AUTHOR INFORMATION

Corresponding Author

*(T.L.) E-mail: tom.leyssens@uclouvain.be.

ORCID

Vanessa K. Seiler: 0000-0003-1058-1219

Nikolay Tumanov: 0000-0001-6898-9036

Benoit Champagne: 0000-0003-3678-8875

Author Contributions

The manuscript was written through contributions of all authors. All authors have given approval to the final version of the manuscript.

Funding

This work was published thanks to funding of "Actions de Recherche Concertées (ARC 15/20-068) de la direction générale de L'Enseignement non obligatoire et de la Recherche scientifique − Direction de la Recherche scientifique − Communauté française de Belgique" and "Le Fonds de la Recherche Scientifique − FNRS".

Notes

The authors declare no competing financial interest.

■ ACKNOWLEDGMENTS

The authors would like to thank Dominik Cinčić for fruitful discussions. J.W. and N.T. acknowledge financial support from UNamur for running the PC2 technological platform.

■ REFERENCES

(1) Desiraju, G. R. Crystal Engineering: A Holistic view. *Angew. Chem., Int. Ed.* **2007**, *46*, 8342−8356.

(2) Aakeröy, C. B.; Salmon, D. J. Building co-crystals with molecular sense and supramolecular sensibility. *CrystEngComm* **2005**, *7*, 439−448.

(3) Almarsson, Ö.; Zaworotko, M. J. Crystal engineering of the composition of pharmaceutical phases. Do pharmaceutical co-crystals represent a new path to improved medicines? *Chem. Commun.* **2004**, 1889−1896.

(4) Tilborg, A.; Norberg, B.; Wouters, J. Pharmaceutical salts and cocrystals involving amino acids: A brief structural overview of the state-of-art. *Eur. J. Med. Chem.* **2014**, *74*, 411−426.

(5) Sokolov, A. N.; Friščić, T.; MacGillivray, L. R. Enforced Face-to-Face Stacking of Organic Semiconductor Building Blocks within Hydrogen-Bonded Molecular Cocrystals. *J. Am. Chem. Soc.* **2006**, *128*, 2806−2807.

(6) Luscombe, N. M.; Laskowski, R. A.; Thornton, J. M. Amino acid-base interactions: a three-dimensional analysis of protein-DNA interactions at an atomic level. *Nucleic Acids Res.* **2001**, *29*, 2860−2874.

(7) (a) Bučar, D. K.; Filip, S.; Arhangelskis, M.; Lloyd, G. O.; Jones, W. Advantages of mechanochemical cocrystallisation in the solid-state chemistry of pigments: Colour-tuned fluorescein cocrystals. *CrystEngComm* **2013**, *15*, 6289−6291.

(8) Yan, D.; Delori, A.; Lloyd, G. O.; Friščić, T.; Day, G. M.; Jones, W.; Lu, J.; Wei, M.; Evans, D. G.; Duan, X. A cocrystal strategy to tune the luminescent properties of stilbene-type organic solid-state materials. *Angew. Chem., Int. Ed.* **2011**, *50*, 12483−12486.

(9) Carletta, A.; Buol, X.; Leyssens, T.; Champagne, B.; Wouters, J. Polymorphic and Isomorphic Cocrystals of a N-Salicylidene-3-aminopyridine with Dicarboxylic Acids: Tuning of Solid-State Photo- and Thermochromism. *J. Phys. Chem. C* **2016**, *120*, 10001−10008.

(10) Sliwa, M.; Létard, S.; Malfant, I.; Nierlich, M.; Lacroix, P. G.; Asahi, T.; Masuhara, H.; Yu, P.; Nakatani, K. Design, Synthesis, Structural and Nonlinear Optical Properties of Photochromic Crystals: Toward Reversible Molecular Switches. *Chem. Mater.* **2005**, *17*, 4727−4735.

(11) Hadjoudis, E.; Mavridis, I. M. Photochromism and thermochromism of Schiff bases in the solid state: structural aspects. *Chem. Soc. Rev.* **2004**, *33*, 579−588.

(12) Cohen, M. D.; Schmidt, G. M. J.; Flavian, S. Topochemistry. Part II. The Photochemistry of trans-Cinnamic Acids. *J. Chem. Soc.* **1964**, *0*, 2041−2051.

(13) Amimoto, K.; Kawato, T. J. Photochromism of organic compounds in the crystal state. *J. Photochem. Photobiol., C* **2005**, *6*, 207−226.

(14) Jacquemin, P.-L.; Robeyns, K.; Devillers, M.; Garcia, Y. Photochromism Emergence in N-Salicylidene p-Aminobenzenesulfonate Diallylammonium Salts. *Chem. - Eur. J.* **2015**, *21*, 6832−6845.

(15) Mercier, G. M.; Robeyns, K.; Tumanov, N.; Champagne, B.; Wouters, J.; Leyssens, T. New insights into Photochromic Properties of N-Salicylideneaniline Derivates Using a CoCrystal Engineering Approach. *Cryst. Growth Des.* **2019**, *19*, 5544.

(16) Mercier, G. M.; Robeyns, K.; Leyssens, T. Altering the Photochromic Properties of N-Salicylideneanilines Using a Co-Crystal Engineering Approach. *Cryst. Growth Des.* **2016**, *16*, 3198−3205.

(17) Carletta, A.; Spinelli, F.; D'Agostino, S.; Ventura, B.; Chierotti, M. R.; Gobetto, R.; Wouters, J.; Grepioni, F. Halogen-Bond Effects on the Thermo- and Photochromic Behaviour of Anil-Based Molecular Co-crystals. *Chem. - Eur. J.* **2017**, *23*, 5317−5329.

(18) Johmoto, K.; Sekine, A.; Uekusa, H. Photochromism Control of Salicylideneaniline Derivatives by Acid-Base Co-Crystallization. *Cryst. Growth Des.* **2012**, *12*, 4779−4786.

(19) Hadjoudis, E. Photochromic and Thermochromic Anils. *Mol. Eng.* **1995**, *5*, 301−337.

(20) Milia, F.; Hadjoudis, E.; Seliger, J. Hydrogen bond studies in thermochromic and photochromic N-salicylidene anilines. *J. Mol. Struct.* **1988**, *177*, 191−197.

(21) Crano, J. C.; Guglielmetti, R. J. *Organic Photochromic and Thermochromic compounds*; Plenum Press: New York, 1999.

(22) Klajn, R. Spiropyran-based dynamic materials. *Chem. Soc. Rev.* **2014**, *43*, 148.

(23) Berkovic, G.; Krongauz, V.; Weiss, V. Spiropyrans and Spirooxazines for Memories and Switches. *Chem. Rev.* **2000**, *100*, 1741−1753.

(24) Minkin, V. I. Photo-, Thermo-, Solvato-, and Electrochromic Spiroheterocyclic Compounds. *Chem. Rev.* **2004**, *104*, 2751−2776.

(25) Aakeröy, C. B.; Hurley, E. P.; Desper, J.; Natali, M.; Douglawi, A.; Giordani, S. The balance between closed and open forms of spiropyrans in the solid state. *CrystEngComm* **2010**, *12*, 1027−1033.

(26) Görner, H. Photochromism of nitrospiropyrans: effects of structure, solvent and temperature. *Phys. Chem. Chem. Phys.* **2001**, *3*, 416−423.

(27) Celani, P.; Bernardi, F.; Olivucci, M.; Robb, M. A. Conical Intersection Mechanism for Photochemical Ring Opening in

DOI: 10.1021/acs.cgd.9b00903
Cryst. Growth Des. 2020, 20, 608−616

Benzospiropyran Compounds. *J. Am. Chem. Soc.* **1997**, *119*, 10815−10820.
(28) Harada, J.; Kawazoe, Y.; Ogawa, K. Photochromism of spiropyrans and spirooxazines in the solid state: low temperature enhances photocoloration. *Chem. Commun.* **2010**, *46*, 2593−2595.
(29) Seiler, V. K.; Tumanov, N.; Robeyns, K.; Wouters, J.; Champagne, B.; Leyssens, T. A Structural Analysis of Spiropyran and Spirooxazine Compounds and Their Polymorphs. *Crystals* **2017**, *7*, 84−95.
(30) Cavallo, G.; Metrangolo, P.; Milani, R.; Pilati, T.; Priimägi, A.; Resnati, G.; Terraneo, G. The Halogen Bond. *Chem. Rev.* **2016**, *116*, 2478−2601.
(31) Desiraju, G. R.; Ho, P. S.; Kloo, L.; Legon, A. C.; Marquardt, R.; Metrangolo, P.; Politzer, P.; Resnati, G.; Rissanen, K. Definition of the halogen bond (IUPAC Recommendations 2013). *Pure Appl. Chem.* **2013**, *85*, 1711−1713.
(32) Huber, S. M.; Scanlon, J. D.; Jimenez-Izal, E.; Ugalde, J. M.; Infante, I. On the directionality of halogen bonding. *Phys. Chem. Chem. Phys.* **2013**, *15*, 10350−10357.
(33) Seiler, V. K.; Callebaut, K.; Robeyns, K.; Tumanov, N.; Wouters, J.; Champagne, B.; Leyssens, T. Acidochromic spiropyran-merocyanine stabilisation in the solid state. *CrystEngComm* **2018**, *20*, 3318−3327.
(34) Colaço, M.; Carletta, A.; Van Gysel, M.; Robeyns, K.; Tumanov, N.; Wouters, J. Direct Access by Mechanochemistry or Sonochemistry to Protonated Merocyanines: Components of a Four-State Molecular Switch. *ChemistryOpen* **2018**, *7*, 520−526.
(35) Seiler, V. K.; Robeyns, K.; Tumanov, N.; Cinčić, D.; Wouters, J.; Champagne, B.; Leyssens, T. A coloring tool for spiropyrans: Solid-state metal-organic complexation versus salification. *CrystEngComm* **2019**, *21*, 4925.
(36) Brammer, L.; Mínguez Espallargas, G. M.; Libri, S. Combining metals with halogen bonds. *CrystEngComm* **2008**, *10*, 1712−1727.
(37) Rosokha, S. V.; Stern, C. L.; Vinakos, M. K. From single-point to three-point halogen bonding between zinc(II) tetrathiocyanate and tetrabromomethane. *CrystEngComm* **2016**, *18*, 488−495.
(38) Ding, X.; Tuikka, M. J.; Hirva, P.; Kukushkin, V. Yu.; Novikov, A. S.; Haukka, M. Fine-tuning halogen bonding properties of diiodine through halogen-halogen charge transfer - extended [Ru(2,2′-bipyridine)(CO) 2 × 2]·I 2 systems (X = Cl, Br, I). *CrystEngComm* **2016**, *18*, 1987−1995.
(39) Nemec, V.; Fotović, L.; Friščić, T.; Cinčic, D. A large family of halogen-bonded cocrystals involving metal-organic building blocks with open coordination sites. *Cryst. Growth Des.* **2017**, *17*, 6169−6173.
(40) Lisac, K.; Cinčić, D. Simple design for metal-based halogen-bonded cocrystals utilizing the M-Cl···I motif. *CrystEngComm* **2018**, *20*, 5955−5963.
(41) Rigaku Oxford Diffraction *CrysAlisPro Software System*, Version 1.171.37.35; Rigaku Corporation: Oxford, U.K., 2015; Crysalis.
(42) Sheldrick, G. M. Crystal structure refinement with SHELXL. *Acta Crystallogr., Sect. C: Struct. Chem.* **2015**, *71*, 3−8.
(43) Spek, A. L. Structure validation in chemical crystallography. *Acta Crystallogr., Sect. D: Biol. Crystallogr.* **2009**, *65*, 148−155.
(44) Macrae, C. F.; Bruno, I. J.; Chisholm, J. A.; Edgington, P. R.; McCabe, P.; Pidcock, E.; Rodriguez-Monge, L.; Taylor, R.; van de Streek, J.; Wood, P. A. Mercury CSD 2.0 - New features for the visualization and investigation of crystal structures. *J. Appl. Crystallogr.* **2008**, *41*, 466−470.
(45) Aakeröy, C. B.; Baldrighi, M.; Desper, J.; Metrangolo, P.; Resnati, G. Supramolecular hierarchy among halogen-bond donors. *Chem. - Eur. J.* **2013**, *19*, 16240−16247.
(46) Maharramov, A. M.; Mahmudov, K. T.; Kopylovich, M. N.; Pombeiro, A. J. L. *Non-covalent interactions in the Synthesis and Design of New compounds*; Wiley: 2016.
(47) Desiraju, G. R. Supramolecular Synthons in Crystal Engineering-A New Organic Synthesis. *Angew. Chem., Int. Ed. Engl.* **1995**, *34*, 2311−2327.
(48) Allen, F. H.; Lommerse, J. P. M.; Hoy, V. J.; Howard, J. A. K.; Desiraju, G. R. Halogen···O(Nitro) Supramolecular Synthon in Crystal Engineering: A Combined Crystallographic Database and Ab Initio Molecular Orbital Study. *Acta Crystallogr., Sect. B: Struct. Sci.* **1997**, *B53*, 1006−1016.
(49) Groom, C. R.; Allen, F. H. The Cambridge Structural Database in Retrospect and Prospect. *Angew. Chem., Int. Ed.* **2014**, *53*, 662−671.
(50) Pfrunder, M. C.; Micallef, A. S.; Rintoul, L.; Arnold, D. P.; McMurtrie, J. Interplay between the Supramolecular Motifs of Polypyridyl Metal Complexes and Halogen Bond Networks in Cocrystals. *Cryst. Growth Des.* **2016**, *16*, 681−695.
(51) Cavallo, G.; Metrangolo, P.; Pilati, T.; Resnati, G.; Terraneo, G. Tetraphenylphosphonium iodide-1,3,5-trifluoro-2,4,6-triiodobenzene-methanol (3/4/1). *Acta Crystallogr., Sect. E: Struct. Rep. Online* **2013**, *E69*, o865−o866.
(52) Raatikainen, K.; Rissanen, K. Modulation of N···I and $^{+}$N-H···Cl^{-}...I Halogen bonding: Folding, Inclusion, and Self-Assembly of Tri- and Tetraamino Piperazine Cyclophanes. *Cryst. Growth Des.* **2010**, *10*, 3638−3646.
(53) Beyeh, N. K.; Valkonen, A.; Bhowmik, S.; Pan, F.; Rissanen, K. N-Alkyl ammonium resorcinarene salts: multivalent halogen-bonded deep-cavity cavitands. *Org. Chem. Front.* **2015**, *2*, 340−345.
(54) Moniruzzaman, M.; Sabey, C. J.; Fernando, G. F. Photo-responsive polymers: An investigation of their photoinduced temperature changes during photoviscosity measurements. *Polymer* **2007**, *48*, 255−263.

DOI: 10.1021/acs.cgd.9b00903
Cryst. Growth Des. 2020, 20, 608−616